Sensors and Actuators B 230 (2016) 367–373

Contents lists available at ScienceDirect

Sensors and Actuators B: Chemical

journal homepage: www.elsevier.com/locate/snb

Kinetic control of nanocrack formation in a palladium thin film on an elastomeric substrate for hydrogen gas sensing in air

Sungyeon Kim, Byungjin Jang, Jongbin Park, Young-Kook Lee, Hyun-Sook Lee, Sungmee Cho*, Wooyoung Lee*

Department of Materials Science and Engineering, Yonsei University, 50 Yonsei-ro, Seodaemun-gu, Seoul 03722, Republic of Korea

ARTICLE INFO

Article history:
Received 14 August 2015
Received in revised form 17 February 2016
Accepted 19 February 2016
Available online 22 February 2016

Keywords:
Nanocrack
Tensile velocity
Mechanical properties
Hydrogen sensor
Low detection limit

ABSTRACT

We report the effects of various tensile velocities on the nanocrack formation in a Pd thin film on an elastomeric polydimethylsiloxane substrate and its H_2 sensing properties. A tunable nanocrack along the *x* and *y* axes was created by mechanical stretching/compression cycles with varying tensile velocities. From the microstructural analyses, we found that the tensile velocity has a significant effect on the crack density but little effect on the average crack width. The Pd nanogap sensor prepared under a high tensile velocity showed a high performance with a low detection limit of 500 ppm of H_2 in air. Our results indicate that the higher crack density with the narrow nanocrack width (55–100 nm) propagated over the entire film provides the enhanced H_2 sensing properties in air.

1. Introduction

In order to generate structures at the nanoscale, advanced nanopatterning and nanofabrication technologies typically make use of templates in the fields of soft lithography, nanoimprint lithography, and hot embossing. However, there are also lithography-free methods that can create periodic patterns without the use of templates. Wrinkling and cracking are two examples of periodic patterns that occur in stiff films and on elastomeric substrates. These patterns have generated increasing interests for a wide range of practical applications, including photonics [1–4], stretchable electronics [5–9], microfabrication [1,10–16], and flexible sensors [17–22]. The first wrinkle pattern was reported on a 50-μm-thick Au film thermally deposited on a polydimethylsiloxane (PDMS) substrate, where the thermal expansion mismatch between the metal film and the PDMS substrate, caused by cooling the sample surface from 110 °C to room temperature (RT), was used to cause buckling via compressive stresses [10]. Many studies have developed fundamental theories and a variety of experiments aimed at developing multifunctional micro/nanoscale patterns induced by the internal compressive stress [9,23–27]. In contrast, crack patterns are typically formed using the tensile stress. Some studies on crack pattern formation have reported that the crack pattern can be modulated by altering the mechanical stress applied to the metal/polymer bilayers at ambient temperature. The tensile stress can create an array of nanocracks within the stiff film that are perpendicular to the applied stress because of the differences between the mechanical properties of the metal thin film and those of the elastomeric substrate [28].

In our earlier work, we investigated a nanogap-based sensor in a Pd metal film on a PDMS substrate by applying tensile stress for the first time [29]. Subsequently, qualitative methods have been suggested to develop the nanogap-based sensors using both a highly mobile thin film on an elastomeric substrate by stretching [30–32] and a cracked Pd film on an elastomeric substrate by repeat of H_2 treatment for different H_2 concentrations [33,34] for controlling the crack formation for H_2 sensors. The performance of such sensors was tested in inert N_2 environments. The sensors exhibited superior on–off behavior with a wide range of detection H_2 (10–40000 ppm) in N_2 [29–34]. The studies also reveal that the reduction in the crack width is a significant factor for the detection of a low H_2 concentration under N_2 [29–34]. However, many efforts have not been made to create the nanocracks and control its width or density via a quantitative method for nanogap-based sensors used for H_2 sensor in air atmosphere for practical applications.

In this study, we report the effects of various tensile velocities on the nanocrack formation in a Pd thin film on an elastomeric PDMS substrate and its sensing properties in the air. We demonstrate that intentional mechanical stretching/compression cycles provide tunable nanocrack formation along the *x* and *y* axes which can be controlled due to tensile velocity.

* Corresponding author. Fax: +82023125375.
E-mail addresses: wooyoung@yonsei.ac.kr (W. Lee), csmise@yonsei.ac.kr (S. Cho).

http://dx.doi.org/10.1016/j.snb.2016.02.093
0925-4005/

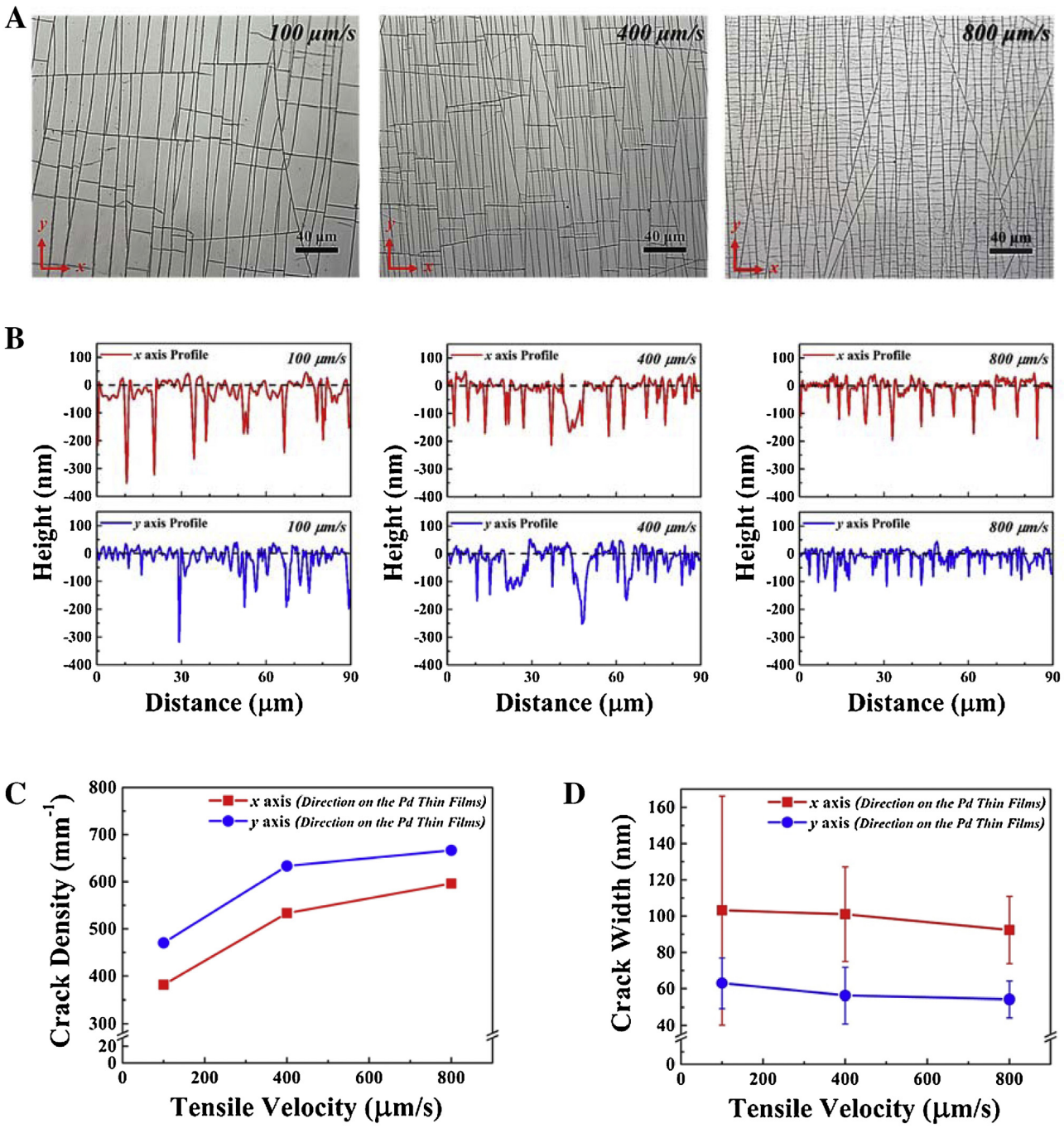

Fig. 1. (A) Perspective-view optical microscopy of nanocracks generated in a Pd thin film on PDMS after applying a tensile stress as a function of the tensile velocity, (B) crack depth distribution along the *x* and *y* axes obtained from the atomic force microscopy (AFM) maps, (C) crack density calculated from the AFM depth profiles at various tensile velocities, and (D) average crack width distribution along the *x* and *y* axes estimated from an SEM images.

2. Experiment

2.1. Fabrication of samples

A thin film of PDMS cured at RT for 16 h and then at 75 °C for 3 h was used as an elastomeric substrate (1.0 cm (W) × 2.7 cm (L), 0.6–0.75 mm thick), and a Pd film was deposited on top of the PDMS substrate via ultrahigh-vacuum (UHV) DC magnetron sputtering in an Ar atmosphere. The Pd film was 1.0 cm (W) × 1.5 cm (L) in area with a thickness of 10 nm. The deposition process was carried out below 2.4×10^{-3} Torr in Ar at a flow rate of 34 sccm in a vacuum chamber with a base pressure of 4.7×10^{-8} Torr. The purity of the Pd target was 3 N. The deposition rate of the Pd film at RT was ~3.7 Å/s at 20 W.

2.2. Nanocrack formation

The mechanical properties of the Pd thin films on PDMS were measured using a microtensile tester (Linkam, TST350) with a force of 10–14 N at constant RT tensile velocities of 100, 400, and 800 μm/s. The samples were strained by 100% over 20 cycles (loading/unloading), which was defined as $(L - L_0)/L_0 \times 100$ (%), where L_0 and L are the initial length and the final length with an applied ten-

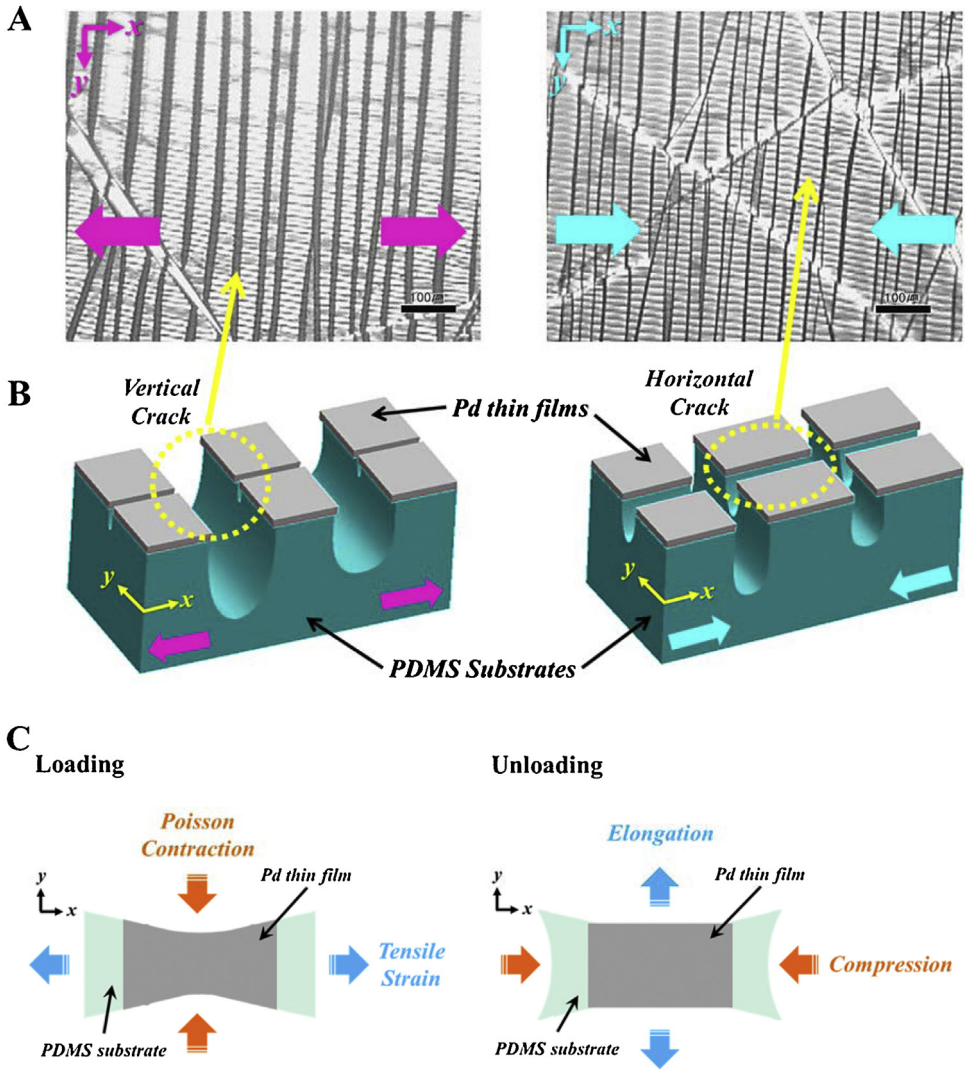

Fig. 2. (A) OM images capturing the nanocrack formation at the top surface of a Pd thin film on PDMS during 100% tensile strain applied with a slow tensile velocity (50 μm/s). (B) Illustrations of crack formation along the *x* and *y* axes at the loading and unloading states to describe the OM images in (A) and (C) Schematic diagrams of the stress distribution in Pd/PDMS during loading/unloading cycles.

sile stress, respectively. Nanocracks were intentionally generated on each sample during repeated cycles at RT.

2.3. Characterization

Following mechanical property testing, scanning electron microscopy (SEM, JEOL JSM-6701F), optical microscopy (OM, Olympus BX41M), and atomic force microscopy (AFM, Park Systems XE-Bio) were used to view both the size of the nanocracks and the surface morphology of the Pd thin film on PDMS. The average nanocracks density were estimated by counting the peaks in the nanocrack depth profiles with the scanning size of (90 μm × 90 μm) obtained at 9 positions in the entire film area (1.0 cm × 1.5 cm).

2.4. Sensor characterization

For the H_2 sensing measurements, the Pd thin film on PDMS was mounted onto a printed circuit board (PCB) and electrically connected to it using Ag paste (P-100, Cans Inc.). The performance of the H_2 sensor was assessed in a gas testing chamber equipped with a mass flow controller (MFC). Sensing properties of the H_2 sensor was measured by monitoring of the change in the resistance in a source-measure unit (Keithley 236, Keithley Instruments Inc.) with a constant voltage supply of 0.1 V for a time interval of 0.1 s. Concentration of H_2 was controlled in the range 500–20,000 ppm in air at RT. A more detailed procedure can be found elsewhere [29].

3. Results and discussion

Images of the nanocracks generated on the Pd thin film on PDMS at different tensile velocities were obtained using OM (Fig. 1A). A significant feature in these images is a creation of the nanocracks along the *y* direction in response to a cyclically applied (20 cycles) uniaxial tensile stress at 100% strain in the *x* direction with depending on the rates of 100, 400, and 800 μm/s. As the tensile velocity is increased, the distance between nanocracks becomes narrower with further crack manipulation in the *x* and *y* directions, indicating that the residual tensile strain creates more crack patterns. More detailed 3D AFM images show the same behavior of the nanocrack pattern observed in OM (Supporting Information, Fig. S1). The nanocrack depth profiles along the *x* and *y* axes under a tensile velocity gradient are shown in Fig. 1B. The nanocrack depths frequently exceeded the Pd film thickness of 10 nm, implying that the cracks expose the underlying substrate. As the tensile velocity is increased, the number of the peaks indicating the crack or buck-

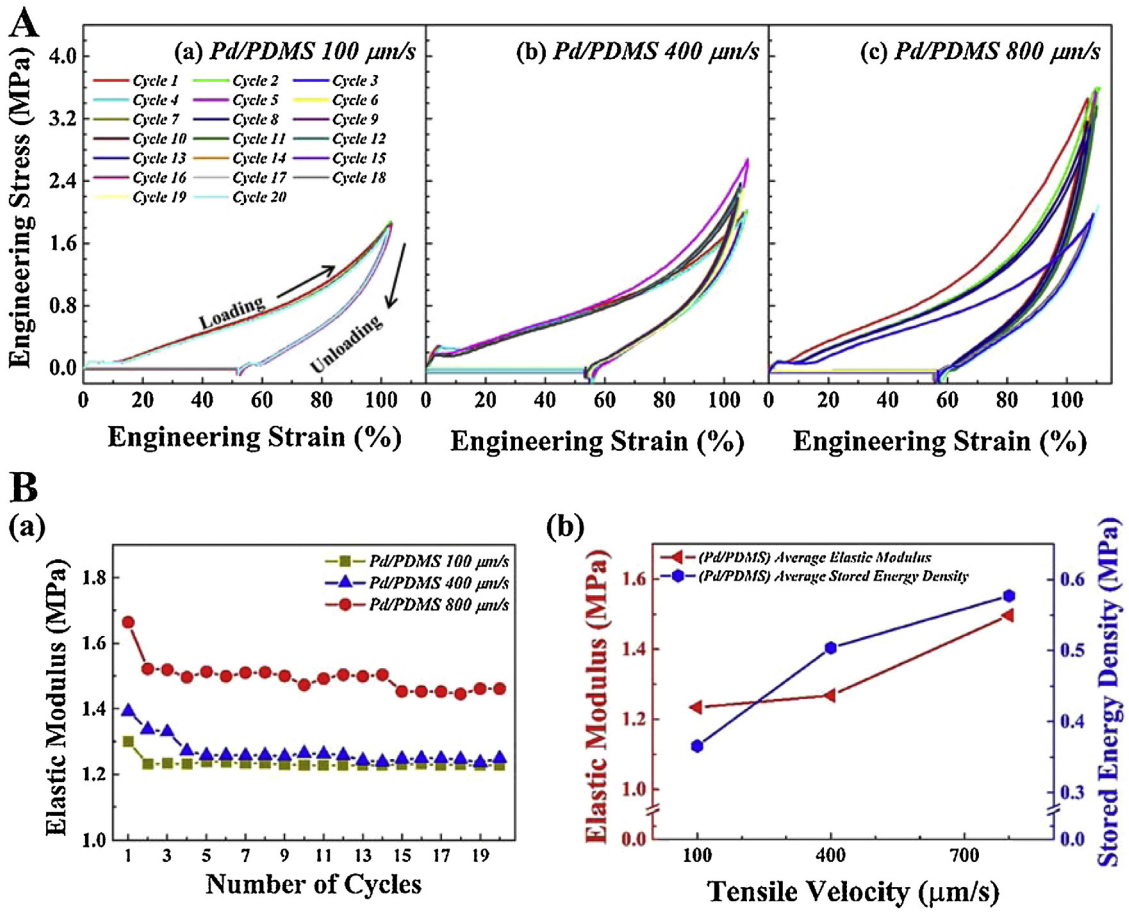

Fig. 3. (A) Stress–strain curves for the Pd thin film on PDMS during 20 loading/unloading cycles with three different tensile velocities of (a) 100, (b) 400, and (c) 800 μm/s. (B) (a) Young's modulus of the Pd/PDMS sample at the 20 cycles repeat for different applied tensile velocities and (b) Average values of elastic modulus and stored energy versus the tensile velocity.

ling are increased. We estimated the average nanocrack density by counting the peaks in the nanocrack depth profiles with the scanning size of 90 μm × 90 μm obtained at 9 positions in the entire film area (1.0 cm × 1.5 cm). The crack density shows an increment with increasing tensile velocity from 100 to 800 μm/s in both directions (Fig. 1C). To evaluate the average nanocrack width, SEM was conducted at 9 positions for each sample (1.0 cm × 1.5 cm), as shown in Supporting Information, Fig. S2. The average nanocrack widths along the *x* and *y* axes in the Pd film are displayed for various tensile velocities in Fig. 1D: 103, 101, and 92 nm along the *x* axis and 63, 56, and 54 nm along the *y* axis for tensile velocities of 100, 400, and 800 μm/s, respectively. It shows no remarkable influence on the magnitude of tensile velocity. Thus, we found that the nanocrack density is strongly governed by the tensile velocity; however, the average nanocrack width has a small effect on the tensile velocity.

Fig. 2A shows OM images of the nanocracks formed in the Pd thin film on PDMS captured at the final state when the stretching is arrived to 100% tensile strain (left of Fig. 2A) and at the beginning state of compression (right of Fig. 2A) with a slow tensile velocity of 50 μm/s. The illustrations representing the OM images in Fig. 2A are exhibited in Fig. 2B. When stretching in the *x* direction, opening of the cracks introduces strong vertical arrays and weak horizontal buckling; then, parallel crack arrays clearly appear when a compressive stress is applied. In contrast, the bare PDMS substrate likely does not have any crack formation (Supporting Information, Fig. S3), despite the high stress applied to the substrate. According to these results, we can predict the mechanism of nanocracks formation in the *x* and *y* directions based on the description in the schematic diagrams in Fig. 2C. When the Pd/PDMS specimen is loaded (unloaded) with applying tensile stress along the *x* axis, extension (compression) and contraction (expansion) occur in *x* axis and *y* axis, respectively. The difference in Poisson ratio ($\nu = -\varepsilon_{yy}/\varepsilon_{xx}$) of relatively stiff Pd metal film and viscoelastic PDMS substrate leads to the different stress distribution on those materials. Therefore, when a tensile stress is applied, perpendicular crack patterns are induced by the applied stress in the *x* direction, and parallel crack patterns are generated during the accompanying compression that occurs in the *y* direction. Controlling the tensile velocity applied to the viscoelastic substrate gives rise to a great variation in the nanocrack area and depth. The residual tensile strain for high velocity generates more opening of the cracks on the top surface. Thus, the development of residual compression/elongation with increased tensile velocity leads to further nanocrack formation in the *x* and *y* directions, even after repeated cycles of stretching and compressing.

Fig. 3A shows the tensile stress versus strain curves of PDMS specimens onto which the thin, 10-nm-thick Pd film was deposited (hereafter, these are called the Pd/PDMS specimens). The flow curves were measured during 20 loading and unloading cycles at RT at three different tensile velocities (100, 400, and 800 μm/s). The stress–strain curves of the Pd/PDMS specimens reveal nonlinear elastic behavior as the bare PDMS does (Supporting Information, Fig. S4B). However, the details are different at higher strain vales. The maximum tensile stress of the bare PDMS (Supporting information, Fig. S4A) is slightly increased with increasing tensile velocity whereas the Pd/PDMS specimen shows significant increase at

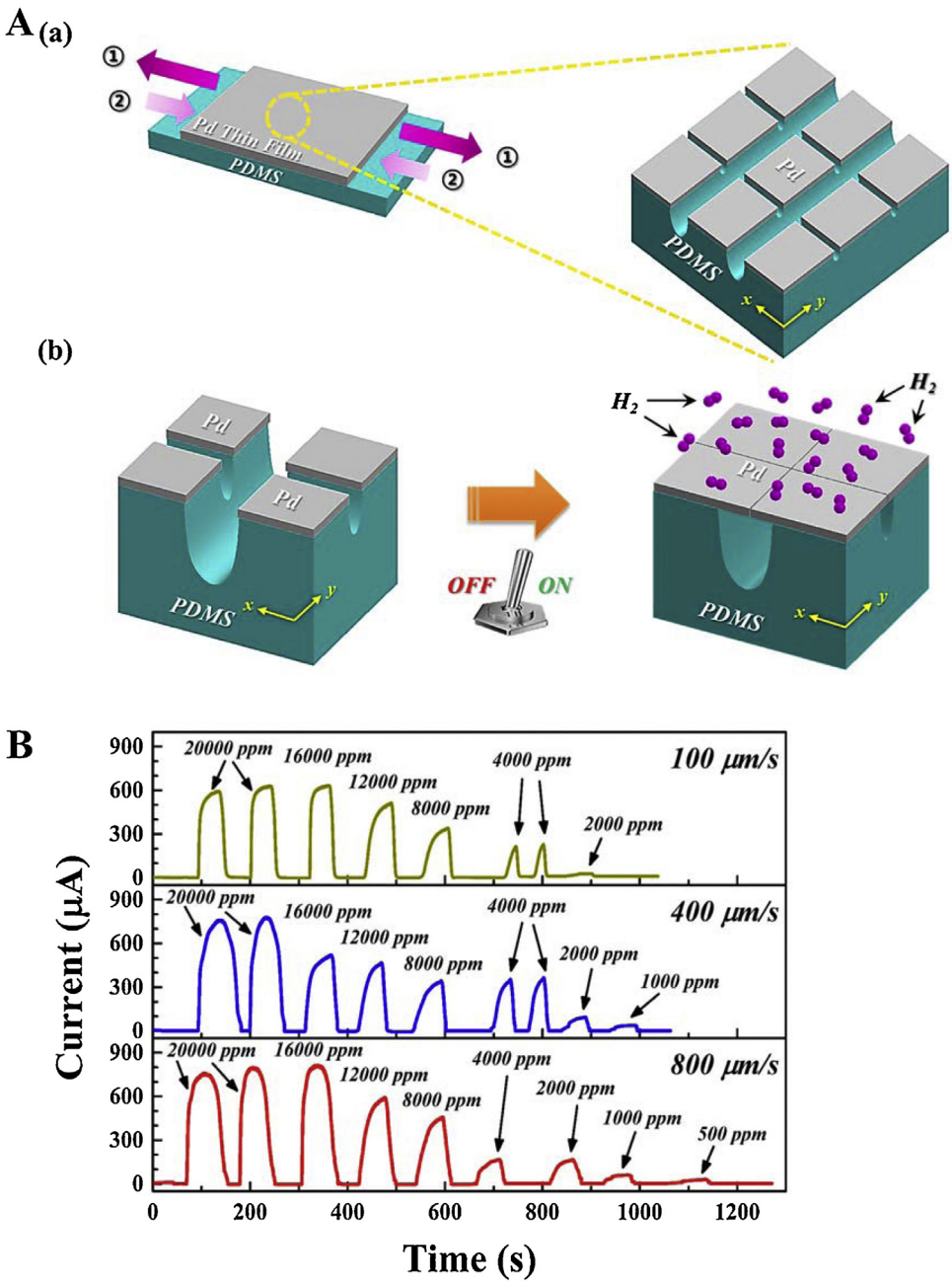

Fig. 4. (A) Schematics of the H_2 sensing procedure using a nanocrack patterned device: (a) crack pattern formation occurring after applying a repeatable ① tensile stress/② compression to the Pd/PDMS sample with three different tensile velocities; nanocracks are generated in the *x* and *y* directions; and (b) connected edges of broken Pd pieces caused by a volumetric change in Pd upon exposure to H_2. (B) The real-time electrical response of the nanocrack patterned device to H_2 versus time in an air carrier at room temperature.

800 μm/s, which is most likely due to strain hardening. The increase in the tensile stress gives an increase in the stored strain energy density (Fig. 3B(b)), which corresponds to the area of the stress versus strain hysteresis loops in Fig. 3A. In addition, the average Young's moduli (Fig. 3B) were calculated from the slopes of the initial linear regions (10–40%) [35,36] of the curves for the Pd/PDMS bilayer with exception of bending characteristics indicated with small hump below 10% strain. A comparison of the Young's moduli implies that the maximum stress experienced in the Pd/PDMS specimen with a high tensile velocity during the loading/unloading cycles (Fig. 3B(b)) was much higher than that in the bare PDMS (Fig. S4B). Thus, the elastic modulus and stored strain energy in the Pd/PDMS specimen increase proportionally with the tensile velocity. This is certainly caused by the mechanical properties of materials; the much thinner Pd metal film (10 nm) and the thick elastomeric PDMS layer (0.6–0.75 mm).

Fig. 4 shows how the H_2 sensing properties across the nanocracks evolve as a function of different tensile velocities. To measure the H_2 sensing capability of nanocracked Pd films on PDMS (Fig. 4A), the following procedure, which is based on our previous study, was used [29]: (i) the Pd thin film on the PDMS substrate was stretched and compressed (100% for each) for 20 cycles using UHV DC sputtering; (ii) the nanocracks were intentionally generated and became deeper and larger in the *x* and *y* directions as the applied tensile velocity increased; (iii) the nanocracked Pd film on PDMS was exposed to hydrogen, leading to a large volume expansion of

Pd with an additional phase transition from the α phase to the β phase, resulting in the formation of palladium hydride; (iv) finally, swelled Pd films were connected with the edges of broken Pd films, and a saturated current was obtained using an applied voltage. The amplitude of the current is related to the H_2 concentration, as is the adjacent current level for H_2 concentrations between 20,000 and 50,000 ppm [37,38]. The H_2 sensing devices' capabilities—the H_2 detection limit and representative electrical resistance versus time—were tested for exposure to H_2 gas in air in the range of 500–20,000 ppm, a realistic range for practical applications. The sensor works a good on–off mode over the entire H_2 concentration range, as shown in Fig. 4B. At 2% H_2 in air, the average response (defined as the time to reach 90% from 10% of the maximum electrical resistance) and recovery (defined as the time to reach 10% from 90% of the baseline resistance) times for the sensors fabricated with three tensile velocities (100, 400, and 800 μm/s) less than 1 s [29,30,32] In principle, when the sensors are exposed to H_2 in air, O_2 molecules react with the Pd film to form chemisorbed O atoms. The result of the H_2 adsorption on the Pd surface leads to the formation of both Pd–H and H_2O based on the following reactions [39]:

$$Pd\text{–}O + 3/2H_2(ads) \rightarrow Pd\text{–}H + H_2O(ads) \quad (1)$$

$$H_2O(ads) \rightarrow H_2O(g) \quad (2)$$

Hence, the rate of the Pd–H formation significantly diminished in air as compared to rate in H_2. An overview of the results shows that the sample prepared using a higher tensile velocity resulted in a relatively low detection limit of 500 ppm of H_2 in air compared to the samples prepared at a low tensile velocity. This is a substantial reduction compared to the detection limit of 12,000 ppm of Pd-film-based nanogap sensor with the wide nanogap (e.g., ~420 nm) in air [32]. Especially, the value is superior to 6000 ppm of the Pd-PMMA hybrid nanogap sensors (Pd film sandwiched between PMMA layers) attributed to an easy H_2 permeation through the PMMA layers [32]. This is primarily due to many narrow nanocracks formed in the Pd film, which rapidly combine owing to the volume expansion of Pd when exposed to hydrogen. Thus, the sensor with a higher density of narrow nanocracks (e.g., 54 and 92 nm along the *x* and *y* axes, respectively, Fig. 1D) leads to a dramatically lower detection limit of 500 ppm H_2 in air. This lower detection limit is strongly derived from the geometrical modification of the nanocracks with variable tensile velocities over the entire Pd film, which is expected, given that it leads to enhanced sensing properties.

4. Conclusions

We demonstrated a newly tuned nanocrack patterning technique by applying kinetic control using various tensile velocities in a Pd metal film on PDMS for H_2 sensor operating at the wide range of detection limit of 500–20,000 ppm in the air. The microstructural analysis using SEM and AFM gives a valuable information about that the density and average width of nanocracks. The crack density grown along the *x* and *y* direction of the specimens is strongly affected by the tensile velocity. However, the average crack width is almost constant with the size of 55–100 nm. A notable feature was found: the significantly enhanced H_2 sensing properties with low detection limit of 500 ppm in air is surely provided from the higher crack density with a narrow nanocrack width of 55–100 nm. Such tunable nanocrack formation provides many new areas of research in flexible electronics and sensor applications.

Acknowledgments

This work was supported by the Priority Research Centers Program through the National Research Foundation of Korea (NRF) (2009-0093823).

Appendix A. Supplementary data

Supplementary data associated with this article can be found, in the online version, at http://dx.doi.org/10.1016/j.snb.2016.02.093.

References

[1] W.H. Koo, S.M. Jeong, F. Araoka, K. Ishikawa, S. Nishimura, T. Toyooka, H. Takezoe, Light extraction from organic light-emitting diodes enhanced by spontaneously formed buckles, Nat. Photonics 4 (2010) 222–226.
[2] G.S. Jeong, D.-H. Baek, H.C. Jung, J.H. Song, J.H. Moon, S.W. Hong, I.Y. Kim, S.-H. Lee, Solderable and electroplatable flexible electronic circuit on a porous stretchable elastomer, Nat. Commun. 3 (977) (2012) 1–8.
[3] J. Liang, L. Li, X. Niu, Z. Yu, Q. Pei, Elastomeric polymer light-emitting devices and displays, Nat. Photonics 7 (2013) 817–824.
[4] M.S. White, M. Kaltenbrunner, E.D. Głowacki, K. Gutnichenko, G. Kettlgruber, I. Graz, S. Aazou, C. Ulbricht, D.A.M. Egbe, M.C. Miron, Z. Major, M.C. Scharber, T. Sekitani, T. Someya, S. Bauer, N.S. Sariciftci, Ultra-thin highly flexible and stretchable PLEDs, Nat. Photonics 7 (2013) 811–816.
[5] J.A. Rogers, T. Someya, Y. Huang, Materials and mechanics for stretchable electronics, Science 327 (2010) 1603–1607.
[6] F. Xu, W. Lu, Y. Zhu, Controlled 3D buckling of silicon nanowires for stretchable electronics, ACS Nano 5 (2011) 672–678.
[7] J. Yin, J.L. Yagüe, D. Eggenspieler, K.K. Gleason, M.C. Boyce, Deterministic order in surface micro-topologies through sequential wrinkling, Adv. Mater. 24 (2012) 5441–5446.
[8] D. Yu, K. Goh, H. Wang, L. Wei, W. Jiang, Q. Zhang, L. Dai, Y. Chen, Scalable synthesis of hierarchically structured carbon nanotube–graphene fibres for capacitive energy storage, Nat. Nanotechnol. 9 (2014) 555–562.
[9] R.H. Kim, H.J. Kim, I. Bae, S.K. Hwang, D.B. Velusamy, S.M. Cho, K. Takaishi, T. Muto, D. Hashizume, M. Uchiyama, P. André, F. Mathevet, B. Heinrich, T. Aoyama, D.-E. Kim, H. Lee, J.-C. Ribierre, C. Park, Non-volatile organic memory with sub-millimetre bending radius, Nat. Commun. 5 (3583) (2014) 1–12.
[10] N. Bowden, S. Brittain, A.G. Evans, J.W. Hutchinson, G.M. Whitesides, Spontaneous formation of ordered structures in thin films of metals supported on an elastomeric polymer, Nature 393 (1998) 146–149.
[11] C.M. Stafford, C. Harrison, K.L. Beers, A. Karim, E.J. Amis, M.R. Van Landingham, H.-C. Kim, W. Volksen, R.D. Miller, E.E. Simonyi, A buckling-based metrology for measuring the elastic moduli of polymeric thin films, Nat. Mater. 3 (2004) 545–550.
[12] K.E. Fimenko, M. Rackaitis, E. Manias, A. Vaziri, L. Mahadevan, J. Genzer, Nested self-similar wrinkling patterns in skins, Nat. Mater. 4 (2005) 293–297.
[13] W. Wu, X. Wen, Z.L. Wang, Taxel-addressable matrix of vertical-nanowire piezotronic transistors for active and adaptive tactile imaging, Science 340 (2013) 952–957.
[14] J.Y. Chung, T.Q. Chastek, M.J. Fasolka, H.W. Ro, C.M. Stafford, Quantifying residual stress in nanoscale thin polymer films via surface wrinkling, ACS Nano 3 (2009) 844–852.
[15] C. Yu, K. O'Brien, Y.-H. Zhang, H. Yu, H. Jiang, Tunable optical gratings based on buckled nanoscale thin films on transparent elastomeric substrates, Appl. Phys. Lett. 96 (2010) 041111.
[16] Y. Xuan, X. Guo, Y. Cui, C. Yuan, H. Ge, B. Cui, Y. Chen, Crack-free controlled wrinkling of a bilayer film with a gradient interface, Soft Matter. 8 (2012) 9603–9609.
[17] H. Jiang, D.-Y. Khang, J. Song, Y. Sun, Y. Huang, J.A. Rogers, Finite deformation mechanics in buckled thin films on compliant supports, Proc. Natl. Acad. Sci. U. S. A. 104 (2007) 15607–15612.
[18] S.C.B. Mannsfeld, B.C.K. Tee, R.M. Stoltenberg, C.V.H.H. Chen, S. Barman, B.V.O. Muir, A.N. Sokolov, C. Reese, Z. Bao, Highly sensitive flexible pressure sensors with microstructured rubber dielectric layers, Nat. Mater. 9 (2010) 859–864.
[19] A.P.A. Raju, A. Lewis, B. Derby, R.J. Young, I.A. Kinloch, R. Zan, S. Novoselov, Wide-area strain sensors based upon graphene-polymer composite coatings probed by Raman spectroscopy, Adv. Funct. Mater. 24 (2014) 2865–2874.
[20] T. Yamada, Y. Hayamizu, Y. Yamamoto, Y. Yomogida, A. Izadi-Najafabadi, D.N. Futaba, K. Hata, A stretchable carbon nanotube strain sensor for human-motion detection, Nat. Nanotechnol. 6 (2011) 296–301.
[21] C. Pang, G.-Y. Lee, T.-i. Kim, S.M. Kim, H.N. Kim, S.-H. Ahn, K.-Y. Suh, A flexible and highly sensitive strain-gauge sensor using reversible interlocking of nanofibers, Nat. Mater. 11 (2012) 795–801.
[22] P. Kim, M. Abkarian, H.A. Stone, Hierarchical folding of elastic membranes under biaxial compressive stress, Nat. Mater. 10 (2011) 952–957.
[23] J. Lee, S. Kim, J. Lee, D. Yang, B.C. Park, S. Ryu, I. Park, A stretchable strain sensor based on a metal nanoparticle thin film for human motion detection, Nanoscale 6 (2014) 11932–11939.
[24] J.G. Son, A.F. Hannon, K.W. Gotrik, A. Alexander-Katz, C.A. Ross, Hierarchical nanostructures by sequential self-assembly of styrene-dimethylsiloxane block copolymers of different periods, Adv. Mater. 23 (2011) 634–639.
[25] N. Bowden, W.T.S. Huck, K.E. Paul, G.M. Whitesides, The controlled formation of ordered, sinusoidal structures by plasma oxidation of an elastomeric polymer, Appl. Phys. Lett. 75 (1999) 2557–2559.
[26] T. Okayasu, H.-L. Zhang, D.G. Bucknall, G.A.D. Briggs, Spontaneous formation of ordered lateral patterns in polymer thin-film structures, Adv. Funct. Mater. 14 (2004) 1081–1088.

[27] L. Pocivavsek, R. Dellsy, A. Kern, S. Johnson, B. Lin, K. Yee, C. Lee, E. Cerda, Stress and fold localization in thin elastic membranes, Science 320 (2008) 912–916.
[28] B.C. Kim, T. Matsuoka, C. Moraes, J. Huang, M.D. Thouless, S. Takayama, Guided fracture of films on soft substrates to create micro/nano-feature arrays with controlled periodicity, Sci. Rep. 3 (3027) (2013) 1–6.
[29] J. Lee, W. Shim, E. Lee, J.S. Noh, W. Lee, Highly mobile palladium thin films on an elastomeric substrate: nanogap-based hydrogen gas sensors, Angew. Chem. Int. Ed. 50 (2011) 5301–5305.
[30] E.Y. Lee, J. Lee, J.-S. Noh, W. Kim, T. Lee, S. Maeng, W. Lee, Pd–Ni hydrogen sponge for highly sensitive nanogap-based hydrogen sensors, Int. J. Hydrog. Energy 37 (2012) 14702–14706.
[31] T. Chang, H. Jung, B. Jang, J. Lee, J.-S. Noh, W. Lee, Nanogaps controlled by liquid nitrogen freezing and the effects on hydrogen gas sensor performance, Sens. Actuators A Phys. 192 (2013) 140–144.
[32] B. Jang, K.-Y. Lee, J.-S. Noh, W. Lee, Nanogap-based electrical hydrogen sensors fabricated from Pd-PMMA hybrid thin films, Sens. Actuators B Chem. 193 (2014) 530–535.
[33] J. Lee, J.-S. Noh, S.-H. Lee, B. Song, H. Jung, W. Kim, W. Lee, Cracked palladium films on an elastomeric substrate for use as hydrogen sensors, Int. J. Hydrog. Energy 37 (2012) 7934–7939.
[34] H. Jung, B. Jang, W. Kim, J.-S. Noh, W. Lee, Ultra-sensitive, one-time use hydrogen sensors based on sub-10 nm nanogaps on an elastomeric substrate, Sens. Actuators B Chem. 178 (2013) 689–693.
[35] K.L. Mills, X. Zhu, S. Takayama, M.D. Thouless, The mechanical properties of a surface-modified layer on polydimethylsiloxane, J. Mater. Res. 23 (2008) 37–48.
[36] R. Lakes, Advances in negative Poisson's ratio materials, Adv. Mater. 5 (1993) 293–296.
[37] F.A. Lewis, The Palladium-Hydrogen System, Academic Press London, New York, 1967.
[38] F.A. Lewis, Hydrogen in palladium and palladium alloys, Int. J. Hydrog. Energy 21 (1996) 461–464.
[39] F. Yang, K.C. Donavan, S.-C. Kung, R.M. Penner, The surface scattering-based detection of hydrogen in air using a platinum nanowire, Nano Lett. 12 (2012) 2924–2930.

Biographies

Sungyeon Kim is a Ph.D. candidate in Department of Materials Science and Engineering at Yonsei University in Korea. She received a B.S. degree in Metallurgical Engineering at Yonsei University in 2005. She currently studies thin film based hydrogen sensors using elastomeric substrates. She is interested in nano-sized electronic materials & devices that especially oxide based semiconductors/display devices/photovoltaics, and sensors.

Byungjin Jang was born in 1987 in Seoul, Republic of Korea. He received a BS degree in Ceramic Engineering at Yonsei University in 2012. He is currently studying MOTIFE sensors using Pd as a step toward his Ph.D. degree in hydrogen sensor devices in Materials Science and Engineering at Yonsei University.

Jongbin Park received his MS degree in Materials Science and Engineering at Yonsei University, Korea in 2015. He is currently studying for improvement of damping capacity in vehicle brake system.

Young-Kook Lee is a professor of Department of Materials Science and Engineering, the director of Research Institute of Iron and Steel Technology at Yonsei University in Korea, and POSCO research professor for automotive steels. He received a BS degree in Metallurgical Engineering in 1987, a MS degree in Metallurgical Engineering in 1989, and Ph.D. degree in Metallurgical Engineering from the Yonsei University, Korea in 1998. His current research is on ferrous metallurgy such as microstructural evaluation, stress analysis, and mechanical properties of thermo-mechanical processed ferrous materials. The research is based upon the thermodynamics, phase transformation, mechanical metallurgy, heat transfer, and so on. Especially, advanced high strength steels (AHSS) for automobiles are studied through computer-aided design. The microstructure and mechanical properties of AHSS steels are investigated through phase transformations, precipitation, internal friction, tensile and fracture behaviors occurring under various temperatures and stresses.

Hyun-Sook Lee received her Ph.D. degree in Physics from Pohang University of Science and Technology (POSTECH) in 2008. She was postdoctoral researcher of Future Convergence Research Division at Korea Institute of Science and Technology (KIST) in Korea. Now she is a research professor to the Institute of Nanoscience and Nanotechnology, Yonsei University. Her research interests are focused on the permanent magnetic materials, solid-state hydrogen storage materials, and superconducting materials.

Sungmee Cho earned her Ph.D. degree in Electrical & Computer Engineering from Texas A&M University in 2011. She was a postdoc researcher in Materials Science and Engineering at Northwestern University in 2011–2012. She has been with Doosan Corporation as a researcher in 2003–2004 and Korea Institute Science Engineering (KIST) as a researcher in 2002–2003 and 2004–2005. Now she is a research professor in Creative Materials Division for BK21 PLUS program of Yonsei University. Her current research interests include Mg_2Si-based thermoelectric (TE) energy conversion, TE module joint, thin film hydrogen storage, hydrogen gas, solid oxide fuel cell (SOFC), and Li ion battery.

Wooyoung Lee is a Professor of Department of Materials Science and Engineering at Yonsei University in Korea. He received a BS degree in metallurgical engineering from the Yonsei University in 1986, an MS degree in metallurgical engineering from the Yonsei University in 1988. He received a PhD degree in Physics from University of Cambridge, England in 2000. He is also the Director, Institute of Nanoscience and Nanotechnology, Yonsei University. In recent years, his research interests have centered on various chemical sensors, thermoelectric materials and devices, quantum transports in nano-devices and novel permanent magnets. He has received a number of awards in nano-related research areas, including a Service Merit Medal (2008) due to contribution on the development of intellectual properties in Korea. He has authored and co-authored over 200 publications, and has edited several special books on nanostructured materials and devices.